# THE Rho/Rac EXCHANGE FACTOR Vav2 CONTROLS NITRIC OXIDE–DEPENDENT RESPONSES IN VASCULAR SMOOTH MUSCLE CELLS

by

**Vincent Sauzeau, María A. Sevilla, María J. Montero and Xosé R. Bustelo**

# SUPPLEMENTAL INFORMATION*

*This file includes:

## (1) SUPPEMENTAL TEXT

### Rac1 is the Vav2 substrate involved in NO–mediated F–actin depolymerization

To identify the Rho/Rac family GTPase working downstream of Vav2 in vSMCs, we compared the translocation of Rac1, Cdc42 and RhoG to the plasma membrane as an indirect read–out of GTPase activation during NO signaling in both wild type and *Vav2*$^{-/-}$ vSMCs. Rac1 was tethered to the plasma membrane of vSMCs upon SNP stimulation, but only when the endogenous Vav2 protein was present (**Supplemental Figure 6**, **A** and **B**). Interestingly, Rac1 activation was induced by SNP but not by BAY41–2272 (**Supplemental Figure 6B**), demonstrating that the NO/Vav2–dependent activation of Rac1 is achieved through an sGC–independent route. We could not observe any detectable translocation of Cdc42 to the membrane upon SNP treatment in *Vav2*$^{+/+}$ or *Vav2*$^{-/-}$ vSMCs (**Supplemental Figure 6A**), indicating that this protein was insensitive to NO signaling. RhoG translocation could not be measured in these studies, because we could not detect this GTPase by immunoblotting of either membrane–enriched fractions or total cell lysates obtained from vSMCs (data not shown). This was probably due to the low expression levels of RhoG in vSMCs (http://symatlas.gnf.org/SymAtlas/). In any case, RhoG did not seem to play any role in this Vav2–dependent pathway, because primary vSMCs from *RhoG*$^{-/-}$ mice (1) reacted to SNP as wild type cells (**Supplemental Figure 6**, **C** and **D**). Thus, these results indicate that Rac1 is probably the Vav2 substrate implicated in this signaling response. Confirming this hypothesis, we observed that the siRNA–mediated knockdown of the *Rac1* transcript (**Supplemental Figure 7A**) mimicked the phenotype of the Vav2 deficiency in vSMCs (**Supplemental Figure 7B**). The siRNA–mediated *RhoA* knockdown

(**Supplemental Figure 7A**) induced F–actin depolymerization in non–stimulated vSMCs (**Supplemental Figure 7B**), further suggesting that the stress fibers present in these cells are maintained through RhoA–mediated signals. Interestingly, the siRNA–mediated depletion of ArhGEF7 (**Supplemental Figure 7A**), a Rac1 GEF involved in the activation of Pak1 in endothelial cells (2), did not induce any defect in the SNP response of vSMCs (**Supplemental Figure 7B**). This result further indicates that the NO–mediated activation of Rac1 in this system is primarily due to the catalytic activity of Vav2.

**Reconstitution of NO signaling using activated forms of Rho/Rac family proteins**

In addition to the PDE5 regulation discussed in the main text, additional experiments indicated that the overexpression of both the rapid cycling Rac1 mutant and wild type Pak1 probably induced vSMC F–actin cytoskeleton disassembly by engaging additional, although marginal, cGMP–independent routes. Thus, we detected that the expression of $Rac1^{F28L}$, but not the GFP alone, elicited a significant depolymerization of the F–actin cytoskeleton in both wild type and *Vav2*$^{-/-}$ cells in the absence of SNP stimulation (**Figure 6**, **A** and **B**; **Supplemental Figure 8**). Since under these conditions PDE5 should not be active in wild type vSMCs, the effect induced by $Rac1^{F28L}$ in the cytoskeleton is probably independent of the inhibition of PDE5 activity. The effect induced by $Rac1^{F28L}$ in the absence of SNP stimulation could be mimicked by the expression in wild type and *Vav2*$^{-/-}$ vSMCs of either $Cdc42^{F28L}$ (**Supplemental Figure 8**) or $Rac1^{F28L+F37A}$ (**Figure 6**, **A** and **B**), two proteins that can bind to, and activate Pak1. Instead, the expression of a Rac1 effector mutant that cannot activate Pak1 ($Rac1^{F28L+Y40}$) was totally ineffective at inducing stress

fiber disassembly in vSMCs in the absence of SNP (**Figure 6**, **A** and **B**). These results suggest that the PDE5– and SNP–unrelated route that mediates the Rac1–dependent disassembly of the F–actin cytoskeleton is also mediated by Pak1. Pak1 has been previously shown to interfere with the activation of $MLC_{20}$ by inducing the phosphorylation–dependent inactivation of MLCK (3–6). This connection is also probably operating in our system, because we have observed that the inhibition of the endogenous MLCK using a chemical drug (1–(5–iodonaphthalene–1–sulfonyl)–1H–hexahydro–1,4–diazepine, also known as ML–7) resulted in an approx. 50% reduction of the F–actin/G–actin ratio in non–stimulated wild type (0.54 ± 0.063 in ML–7 treated versus 1.0 ± 0.047 in ML–7 non–treated cells, $n = 3$) and *Vav2*$^{-/-}$ (0.57 ± 0.042 in ML–7 treated versus 1.0 ± 0.054 ML–7 in non–treated cells, $n = 3$) vSMCs, thus mimicking the effects induced by the ectopic expression of either $Rac1^{F28L}$ or Pak1 in those experimental settings. In any case, whether MLCK or other Pak1 downstream elements are involved in this SNP–independent route remains to be determined. Several observations indicate that this PDE5–unrelated route is playing only marginal roles in the biological process studied in this work. Firstly, this response has been observed only upon expression of constitutively–active versions of Rac1 and Cdc42 GTPases. Secondly, we have observed that the defective disruption of stress fibers in *Vav2*$^{-/-}$ vSMCs is fully rescued by chemically targeting sGC downstream elements (i.e., cGKI, Rock) or by the direct inhibition of PDE5 catalytic activity. These conditions must not target MLCK activity. Finally, these conditions are not directly connected with cGMP level regulation, since the rescue of cGMP generation in *Vav2*$^{-/-}$ vSMCs is only achieved upon SNP stimulation. Hence, under physiological conditions, the

Vav2/Rac1/Pak1 route regulating PDE5 appears to be the main pathway involved in the disassembly of the F–actin cytoskeleton during NO–derived signals.

## (2) SUPPLEMENTAL METHODS

### Protein detection in total cellular lysates, cytosolic and membrane–enriched fractions

To detect proteins in cytosolic and membrane–enriched fractions, total cellular lysates were obtained by homogenizing primary vSMCs in a hypotonic solution containing 20 mM Hepes–KOH (pH 7.4), 10 mM KCl, 10 mM NaCl, 5 mM $MgCl_2$, 1 mM DTT, and a cocktail of protease inhibitors (CØmplete, Roche Molecular Biochemicals). After elimination of cell debri by low–speed centrifugation, lysates were subjected to ultracentrifugation (100,000xg, 1 h, 4°C) to obtain the cytosolic (supernatant) and membrane–enriched fractions (pellet), as previously described (7). For detecting proteins in total cellular lysates, cells of the indicated type were lysed in 10 mM Tris–HCl (pH 8.0), 1% Triton X–100, 150 mM NaCl, 1 mM NaF, 1 mM orthovanadate and CØmplete. Extracts were cleared by low–speed centrifugation and supplemented with an equal volume of 2x SDS–polyacrilamide gel electrophoresis (PAGE) sample buffer. After boiling for 10 min, proteins were separated electrophoretically, transferred to nitrocellulose filters, and subjected to immunoblot analysis with the appropriate primary antibody. Protein/antibody complexes were detected with horseradish peroxidase–linked goat secondary antibodies to either anti–mouse or rabbit immunoglobulins using a chemiluminiscent method (Pierce Biotechnology). Antibodies used in immunoblots included mouse monoclonal antibodies to RhoA (Santa Cruz Biotechnology), Rac1 (BD Biosciences), MLCP (BD Biosciences) and tubulin (Oncogene) as well as rabbit polyclonal antibodies to RhoA phosphorylated on $Ser^{188}$ (Santa Cruz Biotechnology), total $MLC_{20}$ (Cell Signaling Technology), $MLC_{20}$ phosphorylated on Ser 19 (Cell Signaling Technology), and MLCP phosphorylated on Thr

696 (Upstate/Millipore).

**Construction, generation and use of retroviruses**

The fast cycling mutants of Rac1 (F28L), RhoA (F30L) and Cdc42 (F28L) were expressed in vSMCs using retroviruses. To this end, we used derivatives of pMIEG3, a retroviral vector that expresses bicistronically the cloned cDNAs and the EGFP. These plasmids, kindly provided by Dr. Y. Zheng (Cincinnati Children's Hospital Medical Center, Cincinnati, OH), have been described before (8). We used the same retroviral vector to clone the cDNAs encoding wild type Vav2 and Pak1 to generate the retroviral plasmids pVS3 and pVS7, respectively. $Rac1^{F28L+F37A}$ (pVS5)–, $Rac1^{F28L+Y40C}$ (pVS6)–, and kinase–dead Pak1 (K298R mutant, pVS8)–encoding retroviral vectors were generated by site–directed mutagenesis using the QuickChange Site–Directed Mutagenesis Kit (Stratagene) and the respective pMIEG3 constructs as template. Recombinant retroviruses were generated using the packaging Phoenix cell line. To this end, these cells were transfected with 4 μg of the appropriate retroviral vector, 7 μg of a plasmid encoding the viral Gag–pol protein, and 3.5 μg of plasmid encoding the viral Env protein. 48 h after transfection, the culture medium was removed and used to infect primary vSMCs twice in a 24 h period. 48–72 h postinfection, infected vSMCs were subjected to subsequent analyses.

**Determination of Vav2 phosphorylation levels**

Lysates from vSMCs from the indicated culture conditions were obtained as indicated above, cleared by low–speed centrifugation, and incubated with 5 μl of a homemade rabbit

polyclonal antibody to Vav2 antibodies 1 h at 4°C. Immunocomplexes were recovered using protein G–Sepharose beads (GE Healthcare) for 1h at 4°C, washed five times in ice–cold lysis buffer, denatured by boiling in SDS–PAGE sample buffer, fractionated electrophoretically and subjected to immunoblot analysis with anti–phosphotyrosine antibodies (Santa Cruz Biotechnology).

**siRNA knockdown experiments**

A scrambled control siRNA and siRNAs targeting the *Rac1, RhoA* and *Arhgef7* mRNAs were purchased from Dharmacon. siRNAs were transfected into vSMCs using a linear polyethylenimine derivative (jetPEI, PolyPlus–Transfection) according to the manufacturer's instructions. The efficacy of the knockdown and the biological effects of the siRNA expression in vSMCs were studied 48 h after each transfection.

**Co–immunoprecipitation experiments**

vSMC lysates were immunoprecipitated with a rabbit polyclonal antibody to either PDE5 (Cell Signaling Technology) or Pak1 (Zymed). After collection using protein G–Sepharose beads, the immunocomplexes were separated electrophoretically and subjected to immunoblot analysis using anti–PDE5 antibodies. In the case of co–immunoprecipitations with aortas in toto, aortas (three for each time point) were collected and cleaned manually, incubated in a Krebs–Henseleit solution for 30 min and stimulated by SNP (10 μM) for the indicated periods of time. After stimulation, the aortas were rapidly frozen in liquid nitrogen and homogeneized in lysis buffer. After elimination of cell debri by low–speed

centrifugation, lysates were processes as indicated above for vSMCs.

**Protein purification**

EcoRI/NotI cDNA fragments encoding the human PDE5 regions encompassing 1–320, 321–580, and 681–875 amino acids were generated by PCR using as template phPDE5, a mammalian expression vector provided by Dr. A. Friebe (Ruhr–Universität Bochum, Bochum, Germany) (9). Upon digestion, those fragments were ligated into EcoRI/NotI–linearized pGEX–4T3 (Pfizer) to generate pVS28, pVS29 and pVS30, respectively. GST proteins were induced with 0.3 mM IPTG (Sigma) in LB/ampicillin medium for 2 h at 30°C. Upon induction, bacteria were collected by centrifugation, resuspended on ice–cold PBS and lysed by sonication. Cleared lysates were subjected to affinity chromatography using glutathione–Sepharose beads (GE Healthcare) and, after extensive washes, GST proteins eluted using 10 μM glutathione (Sigma) in 50 mM Tris–HCl (pH 8.0). Eluted fractions were pooled, dialyzed against a solution containing 20 mM Tris–HCl (pH 8.0), 10 mM $MgCl_2$ and 1 mM DTT, and concentrated (Amicon Ultra–3K, Millipore). Protein concentrations were determined by SDS–PAGE and Coomassie staining using serial concentrations of bovine serum albumin as standard.

**Pull–down experiments**

2 μg of either GST alone or the indicated GST–PDE5 fusion proteins were mixed with lysates from COS1 cells that had been previously transfected using the DEAE–dextrane method with Pak1–expressing mammalian vectors. Those included pACC22, a pCMV6–

XL5 (Origene)–based expression vector encoding wild type Pak1 tagged at its N–terminus with the Myc epitope; pGFP–Pak1(65–150), a pCEFL–GFP–derived plasmid encoding an EGFP–tagged fragment (residues 65–150) of Pak1 (provided by Dr. J.S. Gutkind, National Institutes of Health, Bethesda, MD) (10) and pCMV5M–Pak1(165–545), a pCMV5M–based vector containing the Myc–tagged C–terminal region (residues 165–545) of Pak1 (provided by Dr. M. Cobb, Southwestern Medical Center, Dallas, TX) (11). After 1 h of incubation at 4°C, the GST proteins were collected using glutathione–Sepharose beads, washed five times with ice–cold lysis buffer, and proteins eluted and denatured by boiling in SDS–PAGE sample buffer. Eluted proteins were analyzed by immunoblots with an anti–Myc antibody (Cell Signaling Technology).

**sGC activity assays**

1 μg of purified sGCα1/β1 (Alexis Biochemicals) was incubated with 150 ng of GST–Pak1 in 50 μl of kinase buffer (20 mM Tris–HCl (pH 8.0), 10 mM $MgCl_2$, 1 mM DTT and 100 μM ATP) for 1 h at 30°C. Then, samples were diluted to obtain an enzyme dilution curve (0.1 to 40 ng) with 3 replicates. For each enzyme dilution, 1 mM GTP (Sigma) with or without 100 μM SNP was added for 20 min at 30°C to each reaction sample. Enzyme reactions were stopped by adding HCl to a final concentration of 0.1 M. Production of cGMP was measured as indicated above.

**(3) SUPPLEMENTAL REFERENCES**

1. Vigorito, E., Bell, S., Hebeis, B.J., Reynolds, H., McAdam, S., Emson, P.C., McKenzie, A., and Turner, M. 2004. Immunological function in mice lacking the Rac–related GTPase RhoG. *Mol Cell Biol* 24:719–729.

2. Stockton, R., Reutershan, J., Scott, D., Sanders, J., Ley, K., and Schwartz, M.A. 2007. Induction of vascular permeability: beta PIX and GIT1 scaffold the activation of extracellular signal–regulated kinase by PAK. *Mol Biol Cell* 18:2346–2355.

3. Sanders, L.C., Matsumura, F., Bokoch, G.M., and de Lanerolle, P. 1999. Inhibition of myosin light chain kinase by p21–activated kinase. *Science* 283:2083–2085.

4. Wirth, A., Schroeter, M., Kock–Hauser, C., Manser, E., Chalovich, J.M., De Lanerolle, P., and Pfitzer, G. 2003. Inhibition of contraction and myosin light chain phosphorylation in guinea–pig smooth muscle by p21–activated kinase 1. *J Physiol* 549:489–500.

5. Hirano, K., Derkach, D.N., Hirano, M., Nishimura, J., and Kanaide, H. 2003. Protein kinase network in the regulation of phosphorylation and dephosphorylation of smooth muscle myosin light chain. *Mol Cell Biochem* 248:105–114.

6. Bokoch, G.M. 2003. Biology of the p21–activated kinases. *Annu Rev Biochem* 72:743–781.

7. Sauzeau, V., Le Jeune, H., Cario–Toumaniantz, C., Smolenski, A., Lohmann, S.M., Bertoglio, J., Chardin, P., Pacaud, P., and Loirand, G. 2000. Cyclic GMP–dependent

protein kinase signaling pathway inhibits RhoA–induced Ca2+ sensitization of contraction in vascular smooth muscle. *J Biol Chem* 275:21722–21729.

8. Guo, F., and Zheng, Y. 2004. Rho family GTPases cooperate with p53 deletion to promote primary mouse embryonic fibroblast cell invasion. *Oncogene* 23:5577–5585.

9. Mullershausen, F., Russwurm, M., Koesling, D., and Friebe, A. 2004. In vivo reconstitution of the negative feedback in nitric oxide/cGMP signaling: role of phosphodiesterase type 5 phosphorylation. *Mol Biol Cell* 15:4023–4030.

10. Gavard, J., and Gutkind, J.S. 2006. VEGF controls endothelial–cell permeability by promoting the beta–arrestin–dependent endocytosis of VE–cadherin. *Nat Cell Biol* 8:1223–1234.

11. Frost, J.A., Steen, H., Shapiro, P., Lewis, T., Ahn, N., Shaw, P.E., and Cobb, M.H. 1997. Cross–cascade activation of ERKs and ternary complex factors by Rho family proteins. *Embo J* 16:6426–6438.

12. Bustelo, X.R. 2008. Vav2. *UCSD Nature Mol Pages*:(DOI: 10.1038/mp.a002361.002301).

13. Bustelo, X.R., and Couceiro, J.R. 2008. Vav3. *UCSD Nature Mol Pages*:(DOI: 10.1038/mp.a002362.002301).

## (4) SUPPLEMENTAL FIGURES AND LEGENDS

**Supplemental Figure 1**
**Sauzeau et al.**

**A**

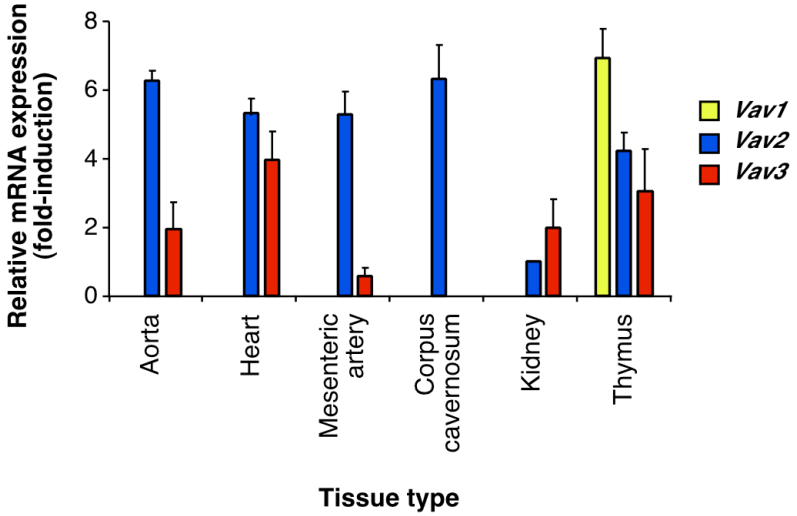


**B**

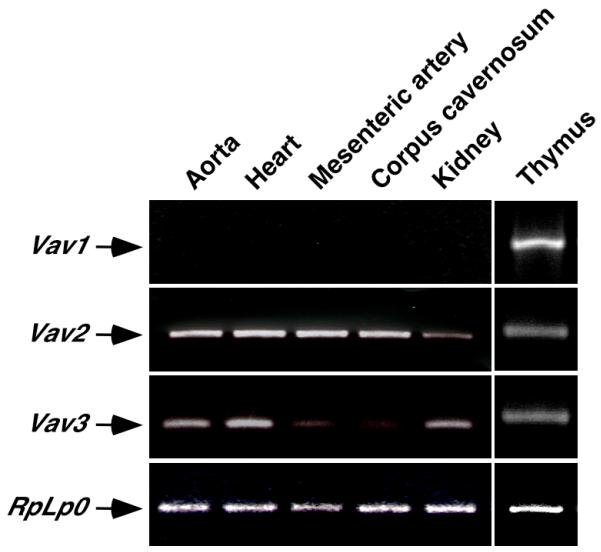

**SUPPLEMENTAL FIGURE 1.** Expression of Vav family members in the cardiovascular system. **(A)** Expression levels determined by quantitative RT–PCR of mRNAs of the indicated *Vav* family genes in aortas, heart, mesenteric artery, corpus cavernossum, kidney, and thymus of four–month–old wild type mice. The latter tissue was included as positive control, since it is known that the three Vav family genes are expressed in this tissue (12, 13). In addition, the expression of the *RpLp0* mRNA in each sample was used an internal control for inter–sample normalization. An arbitrary value of one was given to the expression levels of the Vav2 transcript found in kidney ($n$ = 6–9). **(B)** Aliquots of the final RT–PCR reactions shown above were electrophoretically separated in agarose gels containing ethidium bromide and photographed using a Gel–Doc apparatus (Bio–Rad).

**Supplemental Figure 2**
**Sauzeau et al.**

**A**

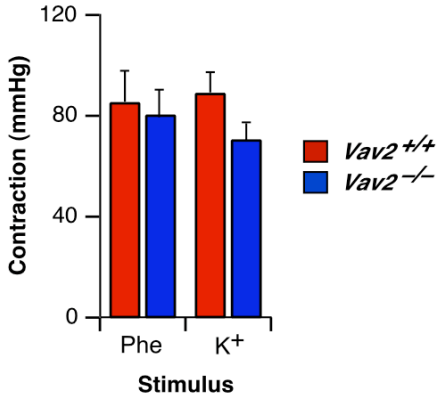


**B**

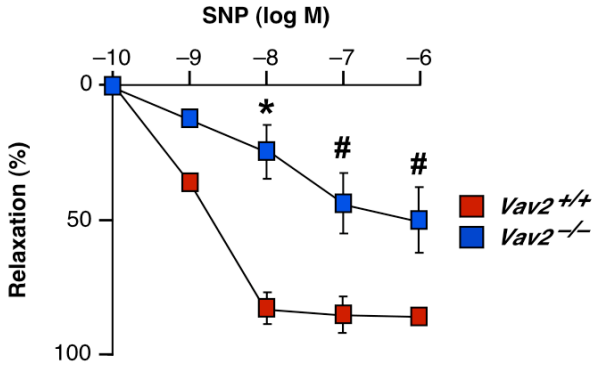


**C**

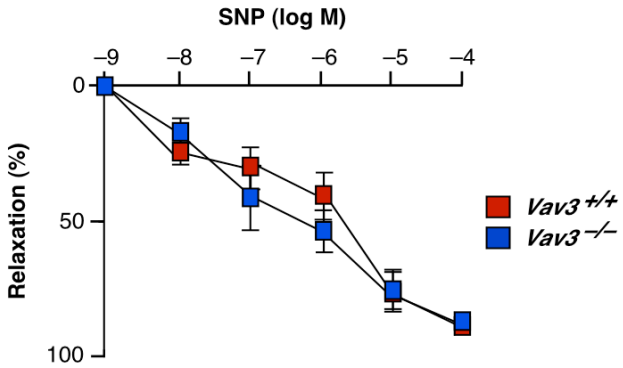

**SUPPLEMENTAL FIGURE 2.** Reactivity of renal arteries from *Vav2*$^{-/-}$ and *Vav3*$^{-/-}$ mice. **(A)** Variation of perfussion pressure induced by Phe and $K^+$ in renal arteries from mice of the indicated genotypes ($n$ = 5–7). **(B,C)** Percentage of vessel relaxation induced by the indicated doses of SNP on Phe–constricted renal arteries from either one–month–old wild type (**B**) and *Vav2*$^{-/-}$ (**B**) ($n$ = 4) or four–month–old wild type (**C**) and *Vav3*$^{-/-}$ (**C**) mice ($n$ = 3). # and ∗ represent $P < 0.05$ and 0.01 compared with wild type controls, respectively. log M, Logarithm of the SNP molar concentration used in each administration.

**Supplemental Figure 3**
**Sauzeau et al.**

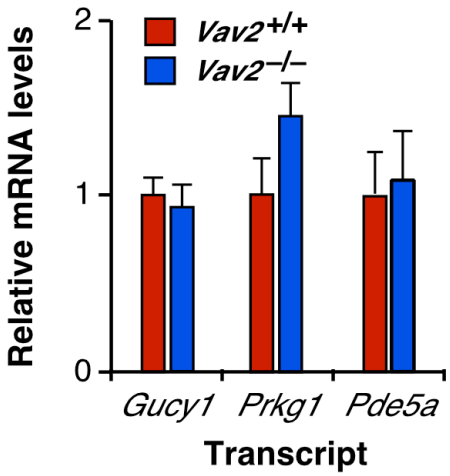


**SUPPLEMENTAL FIGURE 3.** Expression levels of enzymes of the NO–dependent pathway. mRNA levels of *Gucy1* (encoding sGC), *Prkg1* (encoding cGKIα) and *Pde5a* (encoding PDE5a) mRNAs in vSMCs of the indicated genotypes. Expression levels were normalized taking into consideration the *RpLp0* mRNA levels detected in each sample. An arbitrary value of one was given to the expression level of each transcript in wild type vSMCs ($n = 6$).

**Supplemental Figure 4**
**Sauzeau et al.**

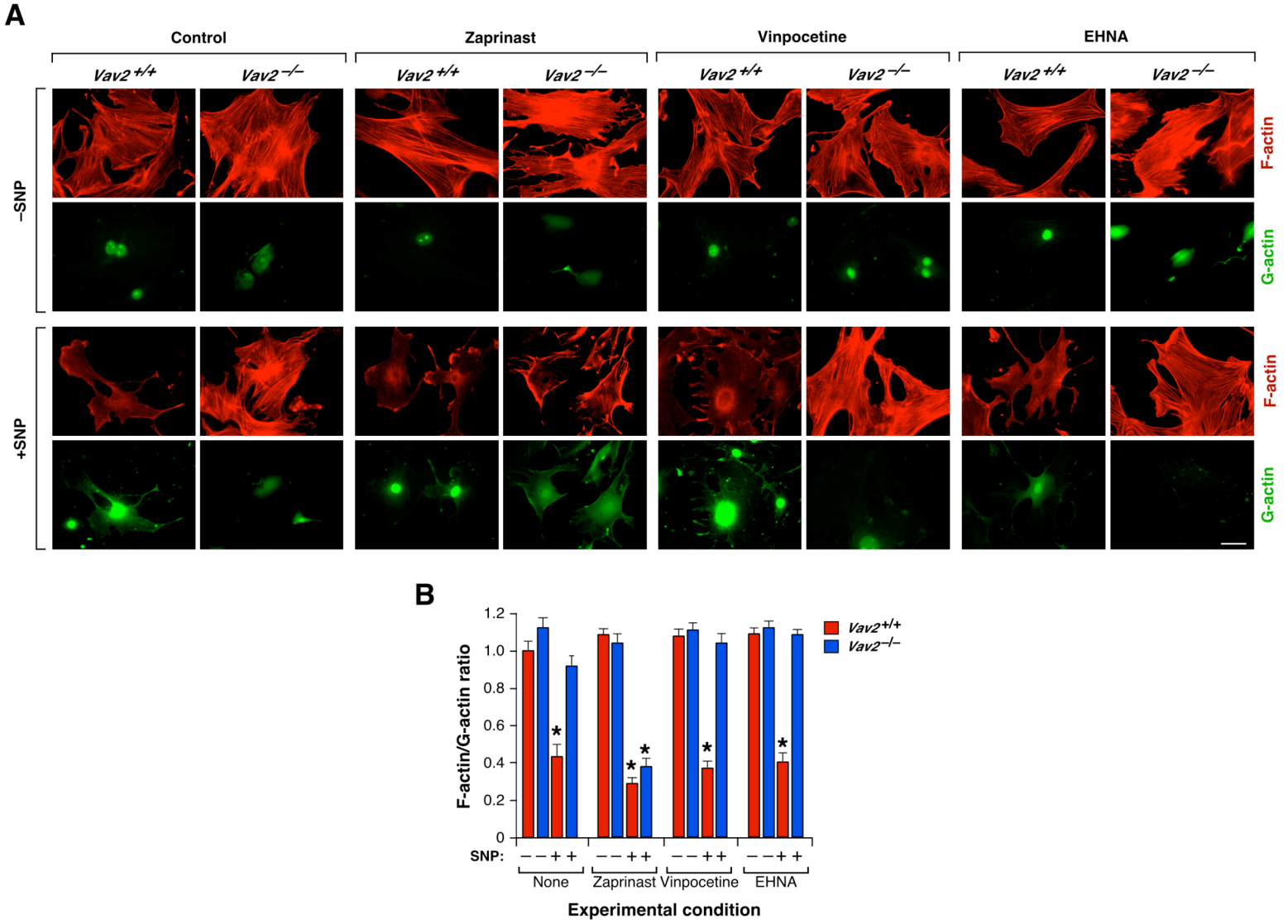

**SUPPLEMENTAL FIGURE 4.** PDE5 inhibitors, but not PDE1 or PDE2 inhibitors, restore normal cytoskeletal responses of *Vav2*$^{-/-}$ vSMCs to NO. **(A)** Representative examples of the status of F–actin (red) and G–actin (green) in wild type and *Vav2*$^{-/-}$ vSMCs treated with or without out SNP (left) and the indicated PDE family inhibitors (top). Scale bar, 20 μm. **(B)** F–actin/G–actin ratio obtained in the above experiments ($n = 3$). ∗, $P < 0.01$ compared with non–stimulated wild type cells (which received an arbitrary value of 1).

**Supplemental Figure 5**
**Sauzeau et al.**

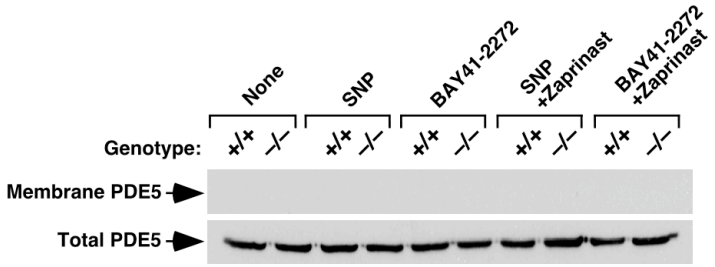


**SUPPLEMENTAL FIGURE 5.** Membrane localization (top panel) and total expression levels (bottom panel) of PDE5 in wild type and *Vav2*$^{-/-}$ vSMCs before (–) and after (+) SNP stimulation for 1 h (top) in the presence or absence of the indicated drugs (top) ($n$ = 2). The samples used in these experiments are aliquots of the same extracts used in **Fig. 3D** (see main text).

**Supplemental Figure 6**
**Sauzeau et al.**

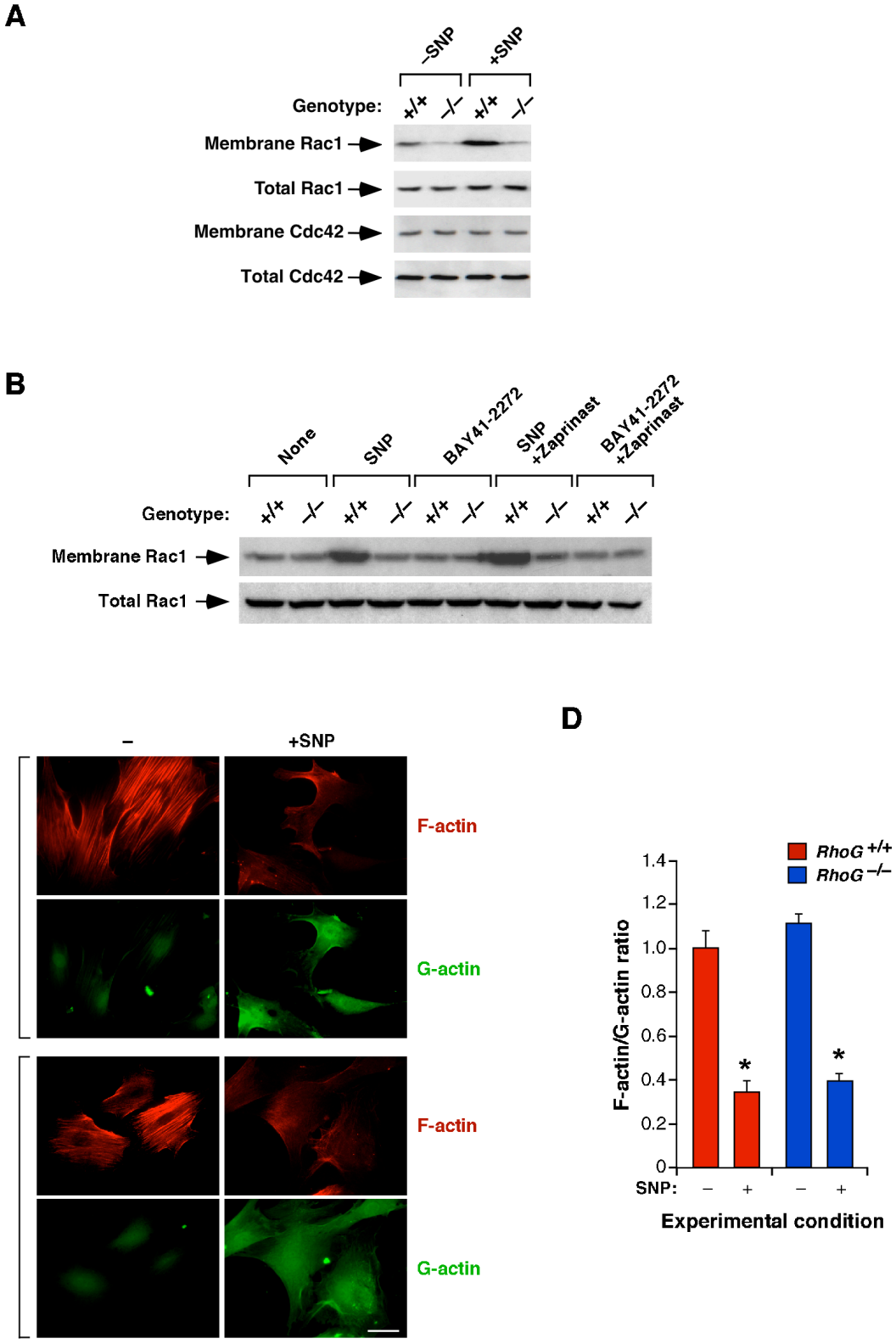

**SUPPLEMENTAL FIGURE 6.** Activation of Rho/Rac family proteins in vSMCs during NO–dependent signaling. **(A,B)** Membrane localization of Rac1 (**A,B**; top panels) and Cdc42 (**A**, third panel from top) as well as total protein levels of Rac1 (**A,B**; second panel from top) and Cdc42 (**A**, bottom panel) in wild type and *Vav2*$^{-/-}$ vSMCs before (–) and after (+) SNP stimulation for 1 h (top). **(C)** Representative images of F–actin (red) and G–actin (green) in vSMCs obtained from wild type and *RhoG*$^{-/-}$ mice (left) that were either non–stimulated (–) or stimulated (+) with SNP (top) for 1 h. Scale bar, 20 μm. **(D)** F–actin/G–actin ratio obtained in the above experiments ($n$ = 3). ∗, $P < 0.01$ compared with non–stimulated wild type controls (which were given an arbitrary value of 1).

**Supplemental Figure 7**
**Sauzeau et al.**

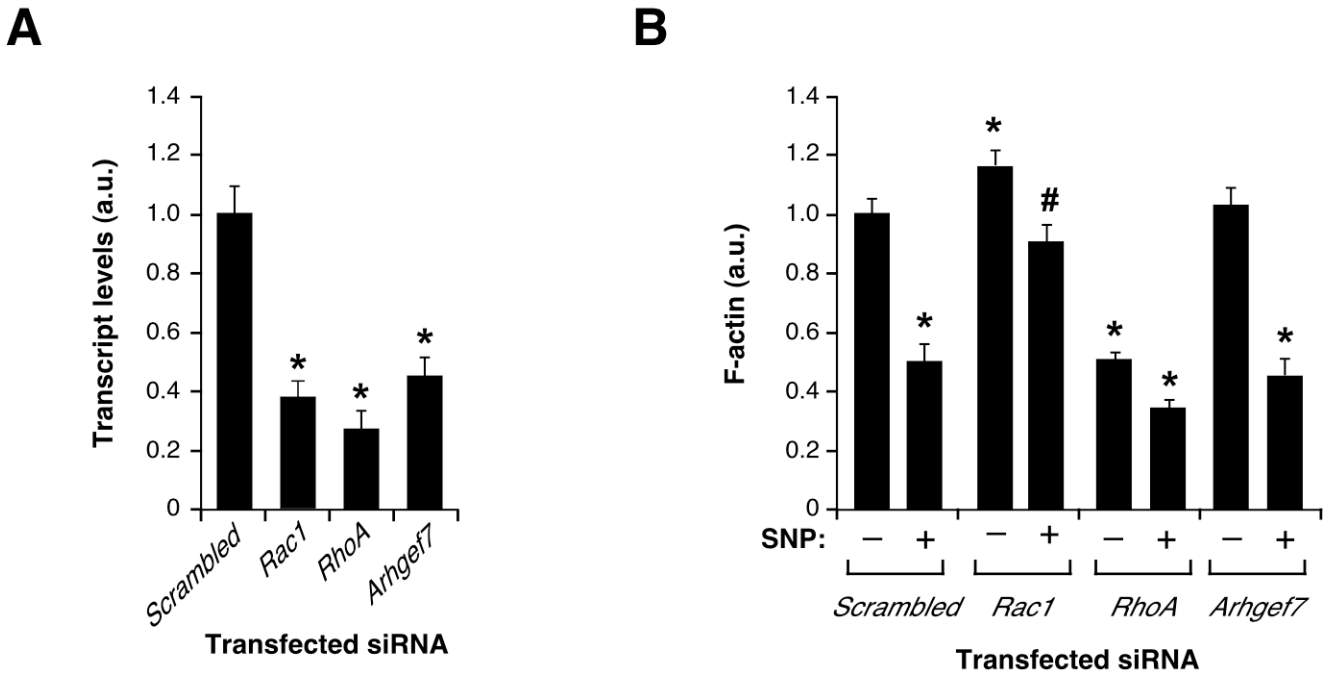

**SUPPLEMENTAL FIGURE 7.** Participation of Rac1 in the NO–dependent responses of vSMCs. **(A)** Wild type vSMCs were transfected with the indicated small interfering RNAs (siRNAs) and the percentage of transcript knowndown after 48 h evaluated by RT–PCR techniques ($n$ = 3). (**B**) Wild type vSMCs were transfected with the indicated siRNAs. After 48 h, cells were stimulated with SNP as indicated, fixed, stained with both rhodamine–conjugated phalloidin and Alexa Fluor488–labeled DNaseI, and the F–actin/G–actin ratio obtained in each experimental condition was evaluated as indicated in Methods. # and ∗ represent, respectively, $P < 0.05$ and 0.01 compared with wild type controls (which were given an arbitrary value of 1).

**Supplemental Figure 8**
**Sauzeau et al.**

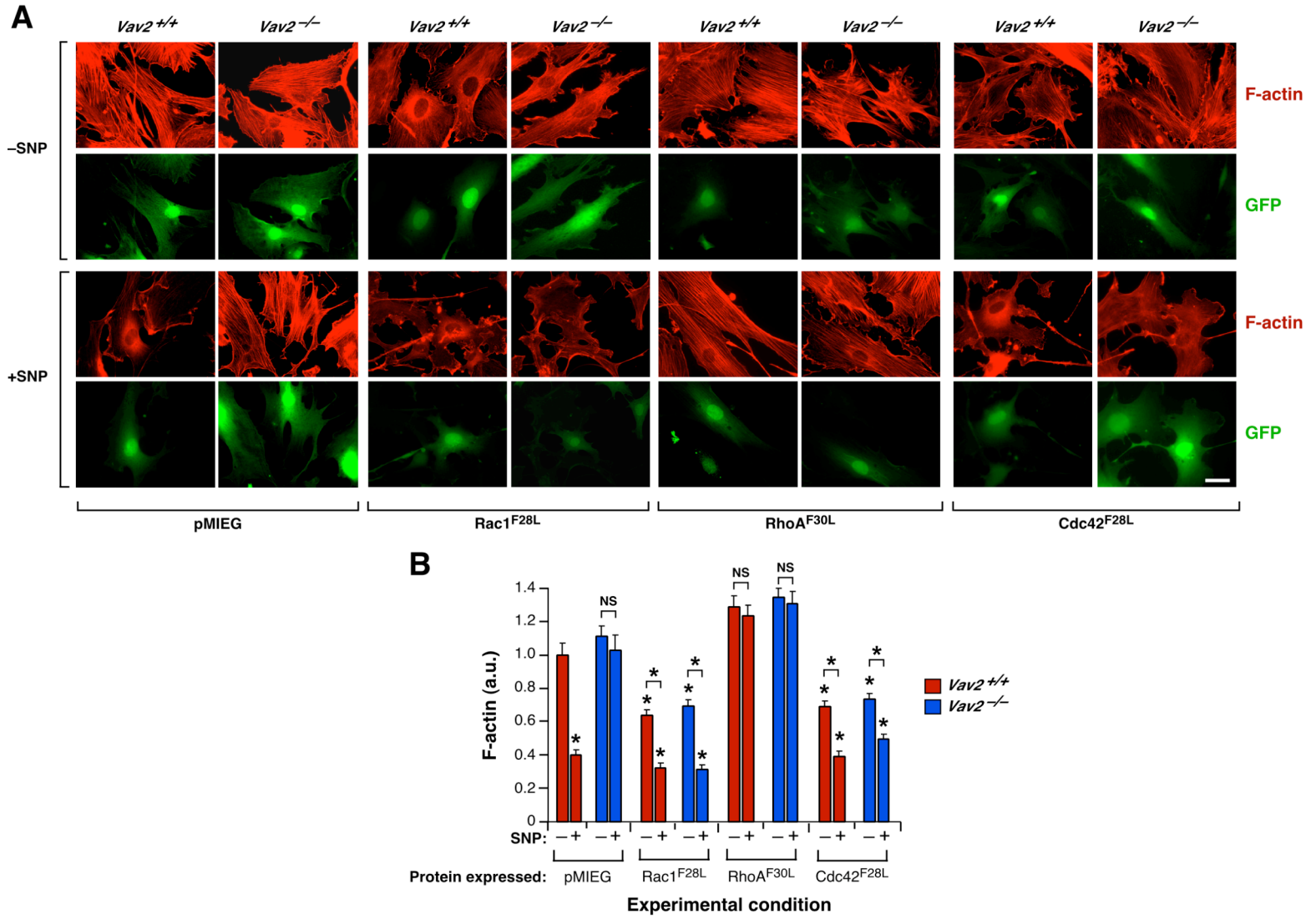

**SUPPLEMENTAL FIGURE 8.** Effect of Rho/Rac family proteins on the F–actin cytoskeleton of vSMCs. **(A)** Representative images of the F–actin cytoskeleton (red) present in non–stimulated (–) and SNP–stimulated (+) wild type and *Vav2*$^{-/-}$ vSMCs previously infected with retrovirus encoding bicistronically GFP (green) and the indicated rapid cycling mutants of Rho/Rac family proteins (bottom). pMIEG refers to the retrovirus encoding only the EGFP protein. Scale bar, 20 μm. **(B)** F–actin levels obtained in the above experiments ($n$ = 3). a.u., arbitrary units. ∗, $P < 0.01$; NS, not significant compared with either non–stimulated wild type control (which was given an arbitrary value of 1) or the indicated not–stimulated cells (brackets).

**Supplemental Figure 9**
**Sauzeau et al.**

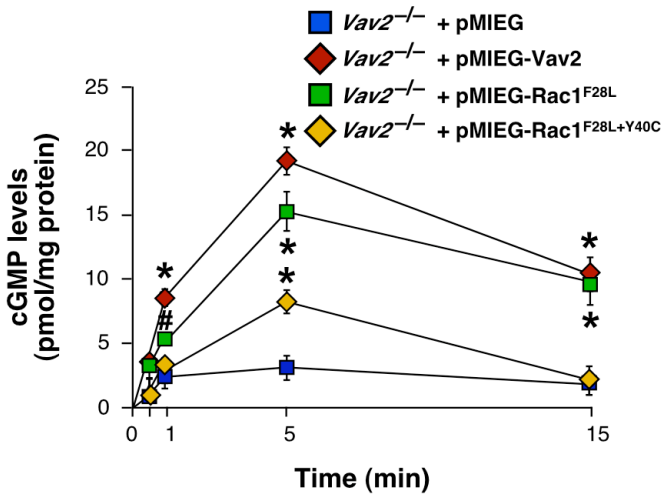


**SUPPLEMENTAL FIGURE 9.** Rac1 restores cGMP production in Vav2–deficient vSMCs. Time–course of cGMP production induced by SNP in *Vav2*$^{-/-}$ vSMCs infected with the indicated retroviruses ($n$ = 2, each performed in triplicate). #, $P < 0.05$; ∗, $P < 0.01$ compared with mock–infected *Vav2*$^{-/-}$ vSMCs.

**Supplemental Figure 10**
**Sauzeau et al.**

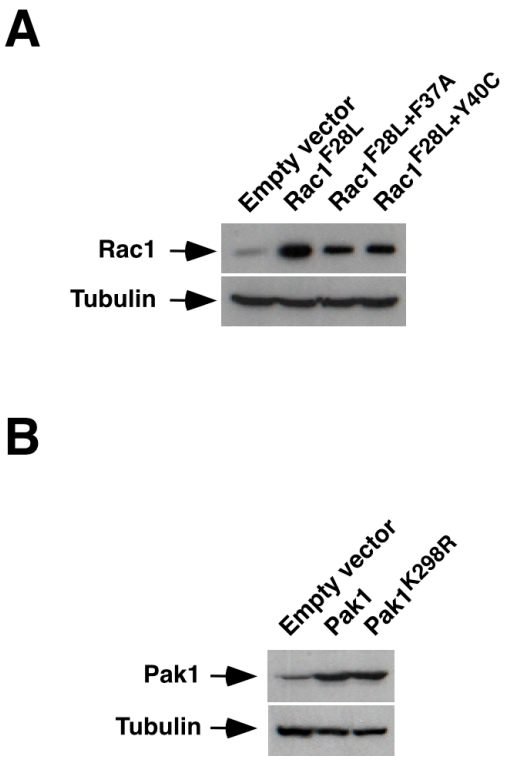


**SUPPLEMENTAL FIGURE 10.** Expression of ectopic proteins in vSMCs. Immunoblot analysis showing the expression of the Rac1 (**A**) and Pak1 (**B**) proteins encoded by the retroviruses used in the vSMC transductions.

**Supplemental Figure 11**
**Sauzeau et al.**

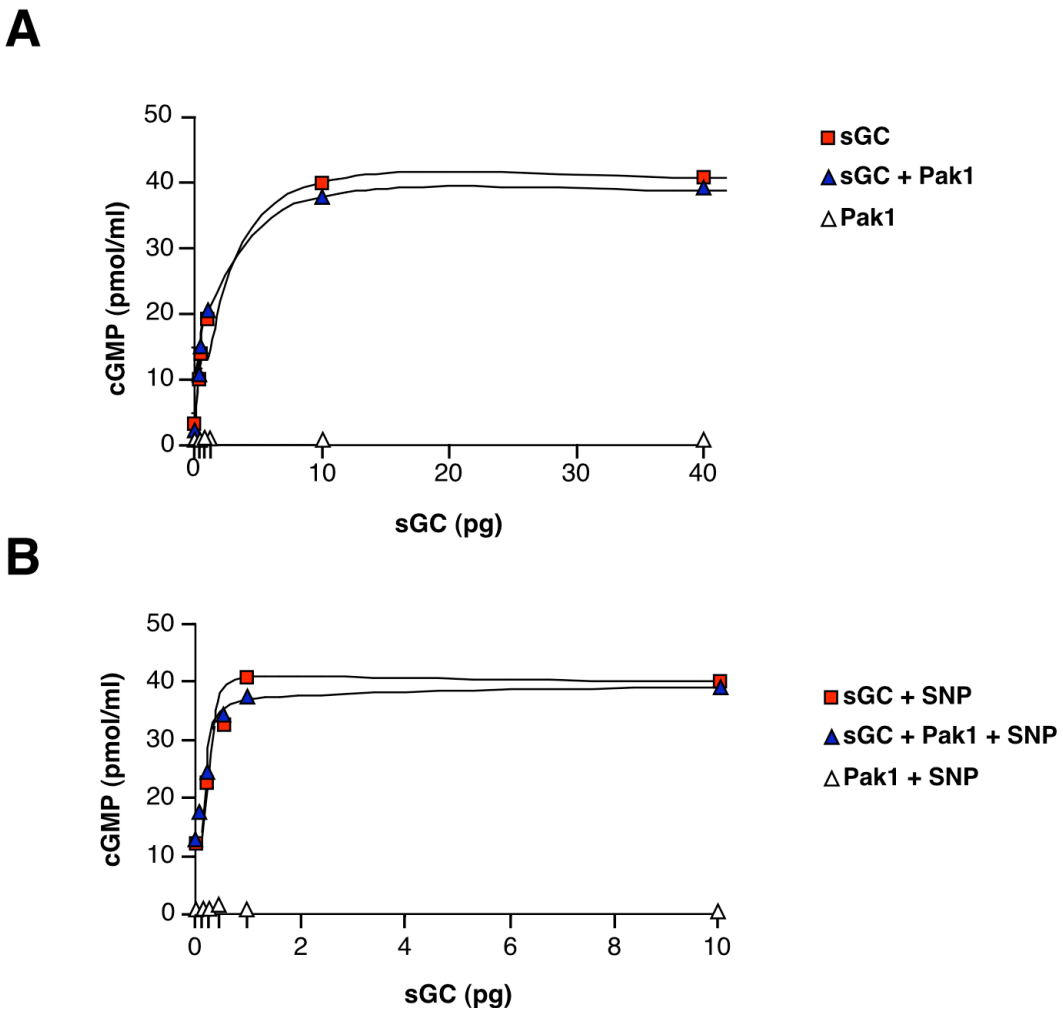


**SUPPLEMENTAL FIGURE 11.** Pak1 does not inhibit sGC. **(A,B)** Kinetics of cGMP production by the cGCα1/β1 complex in the indicated conditions in the basal (**A**) and NO–stimulated (**B**) state.

**Supplemental Figure 12**
**Sauzeau et al.**

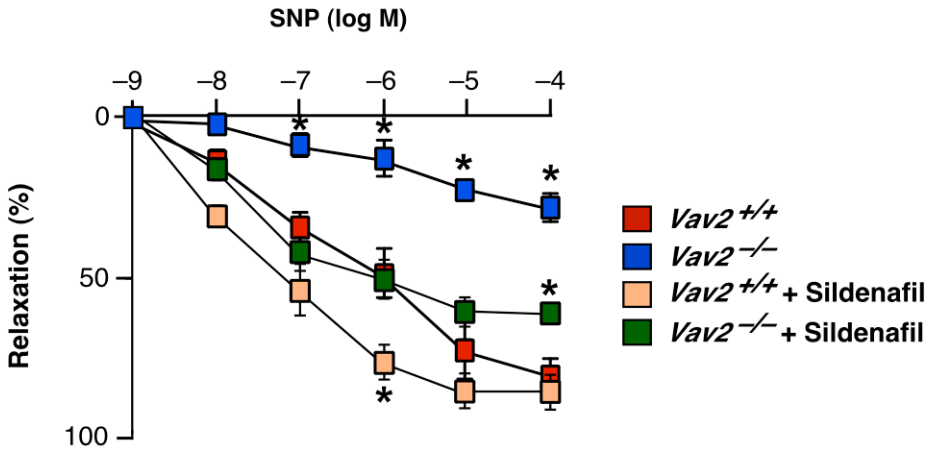


**SUPPLEMENTAL FIGURE 12.** Sildenafil restores the vasodilatation response of *Vav2*$^{-/-}$ renal arteries to NO. 1.5–month–old mice of the indicated genotypes were treated with Sildenafil for 3 months. After this period, the vasodilation response of phenylephrine–constricted renal arteries to SNP was determined as indicated in Methods ($n$ = 4–5 for each genotype). ∗, $P < 0.01$ compared to wild type controls. logM, logarithm of the SNP molar concentration.

**Supplemental Figure 13**
**Sauzeau et al.**

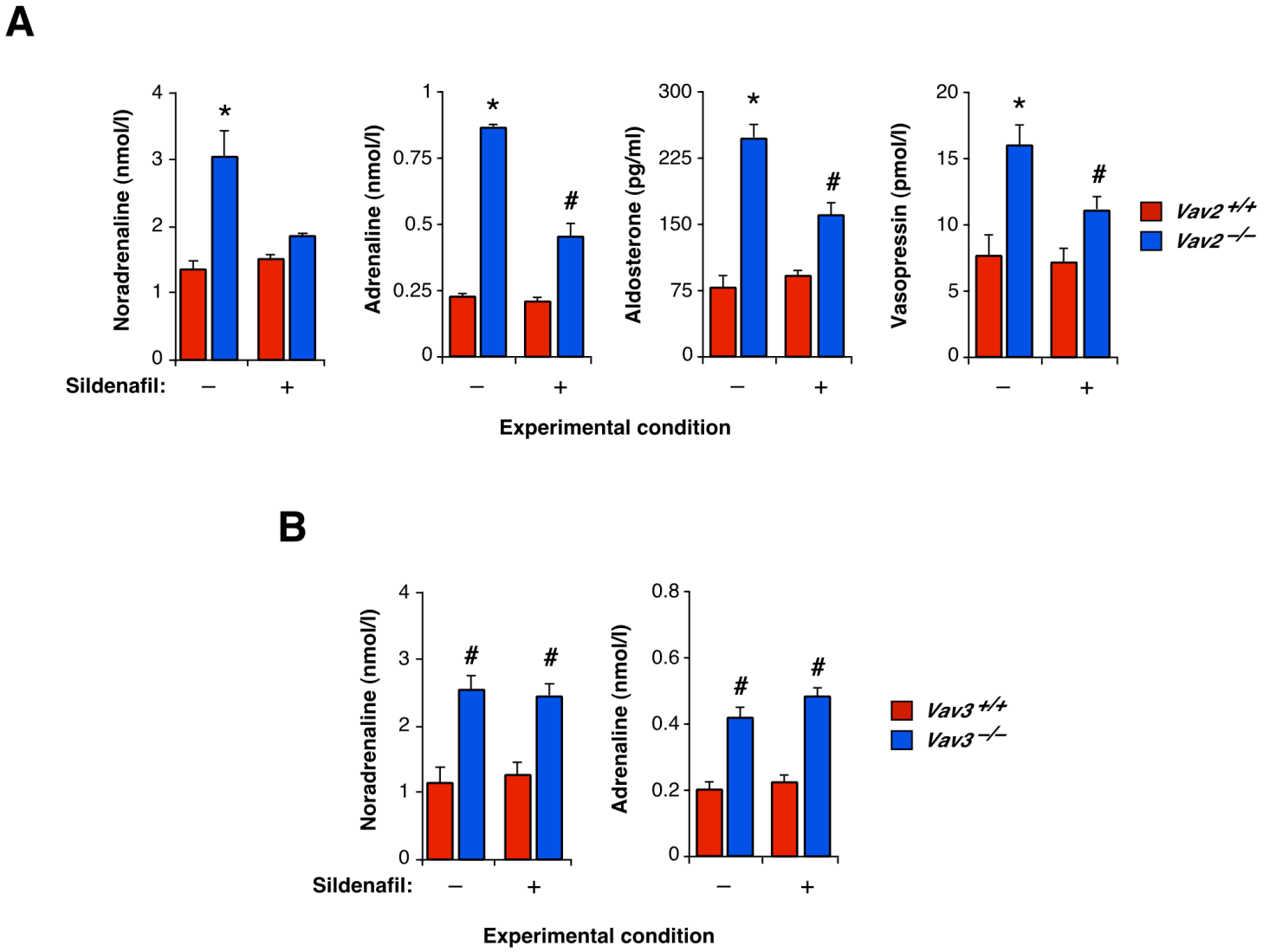

**SUPPLEMENTAL FIGURE 13.** Effect of Sildenafil in other physiological alterations present in Vav2– and Vav3–deficient mice. (**A,B**) Plasma levels of the indicated molecules in wild type (**A,B**), *Vav2*$^{-/-}$ (**A**), and *Vav3*$^{-/-}$ (**B**) mice that were either treated (+) or left untreated (–) with Sildenafil for a total period of three months ($n$ = 4–6). #, $P < 0.05$; ∗, $P < 0.01$ compared with the respective untreated, wild type control.

**Supplemental Figure 14**
**Sauzeau et al.**

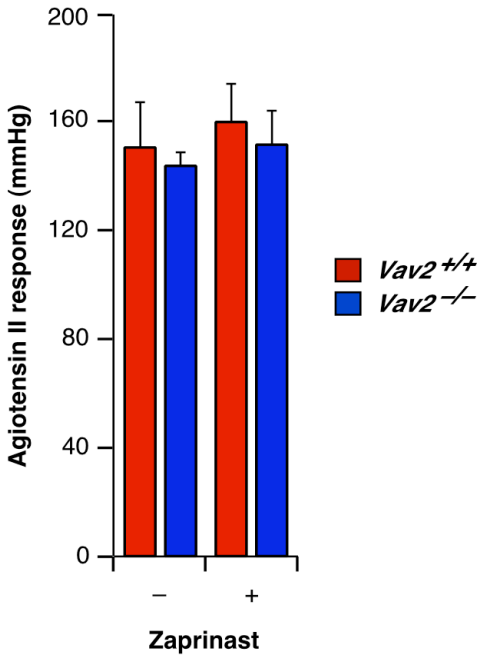


**SUPPLEMENTAL FIGURE 14.** Effect of Zaprinast in angiotensin II–mediated vasoconstriction of renal arteries. Renal arteries from mice of the indicated genotypes were stimulated with angiotensin II (0.1 μM) with (+) or without (–) a preincubation with 10 μM Zaprinast and the variation of perfussion pressure determined as indicated in Methods. Values represent the maximal peak of response in each condition to angiotensin II. $n$ = 6 (experiments with renal arteries from wild type mice in the absence of Zaprinast pretreatments), 7 (experiments with renal arteries from Vav2–deficient mice in the absence of Zaprinast pretreatments), 3 (experiments with renal arteries from wild type mice pretreated with Zaprinast) and 5 (experiments carried out with renal arteries from Vav2–deficient mice pretreated with Zaprinast).